EFFECT OF SPECIMEN THICKNESS AND STRESS RATIO ON FATIGUE CRACK GROWTH AFTER A SINGLE OVERLOAD CYCLE ON STRUCTURAL STEEL

M.Skorupa[1], A. Skorupa[1], J. Schijve[2], T. Machniewicz[1] and P. Korbut[1]

[1]University of Mining & Metallurgy,
Al. Mickiewicza 30, 30-059 Kraków, Poland,
[2]Delft University of Technology,
Kluyverweg 1, P.O.Box 5058, 2600 GB Delft, The Netherlands,

ABSTRACT

Effects of specimen thickness and stress ratio on fatigue crack growth transients after a single overload applied among constant amplitude cycles of a smaller amplitude have been studied experimentally for a low carbon structural steel. The corresponding crack growth data from the fatigue tests have been presented and evaluated. The overload cycles introduced crack growth retardation in all cases and the transient crack growth response depended on a specific combination of specimen thickness and stress ratio. The retardation effect at a given stress ratio decreased as specimen thickness was increased. For a given specimen thickness, the benefit from the overload application was larger at a higher stress ratio than at a lower stress ratio. The test variables predominantly affected crack growth retardation during the period when the crack growth rate was recovering from the minimum value, whilst their effects prior to this minimum (i.e. in the delayed retardation period) were negligible. The observed experimental trends were compared to those reported in the literature for other structural steels.

INTRODUCTION

Since the use of damage tolerance designs became established in many industries, much attention has been devoted to load interaction phenomena in fatigue crack growth which typically occur under variable amplitude load histories. The transient crack growth behaviour following imposition of a single overload (OL) during constant amplitude (CA) cycling of a smaller amplitude is among the most documented load interaction effects. However, as recognized in a recent review study [1], the corresponding data bank for structural steels remains by far more meager than in the case of materials used in the aircraft industry. Especially, the knowledge of the influence of various factors related to loading, material and specimen geometry on OL-induced retardation in crack growth is far from being complete.

This paper examines the effects of specimen thickness (t) and stress ratio (R) on post-OL fatigue crack growth in a low carbon structural steel. The corresponding results of the fatigue crack growth tests are presented and evaluated. A comparison is made between the observed experimental trends and those

reported in the literature for various steels. The work was intended to create an experimental data bank for structural steel required to improve a crack growth prediction model developed by the authors.

EXPERIMENTAL TECHNIQUES

The material used is 18G2A low carbon structural steel, composition 0.14C-1.36Mn-0.21Si-0.020P-0.020S-0.11Cu-0.11Cr-0.05Ni. Mechanical properties in the rolling direction are: yield stress = 392 to 402 MPa, tensile strength = 536 to 544 MPa, and elongation to failure = 22 to 28%. Central crack tension specimens of various thicknesses (Fig. 1) were machined from a 20 mm thick plate with the specimen axis in the rolling direction. Prior to testing, all specimens were stress-relieved.

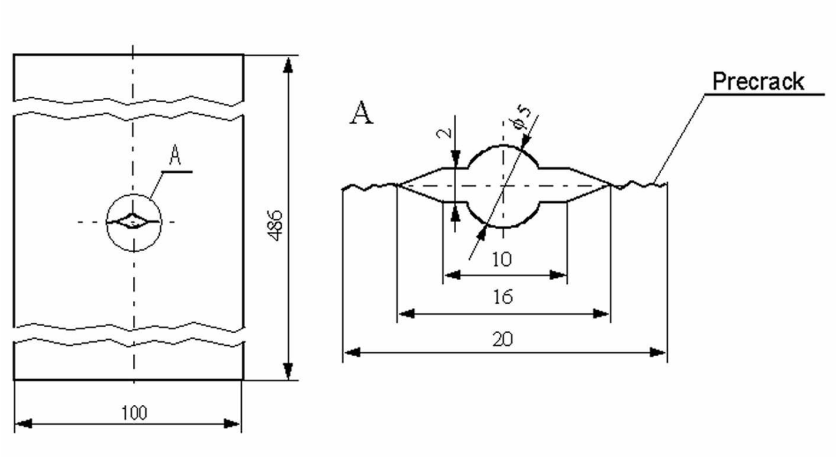

Figure 1: Fatigue specimen geometry, dimensions in mm

All fatigue crack growth tests were performed under load control at 15 to 30 Hz using a Dartec computer-controlled closed-loop servohydraulic fatigue machine with load capacity of 250 kN. A survey of the experiments is given in Table 1. A single 100% OL was always applied at a frequency of 0.1 Hz at the half crack length a_{OL} = 13 mm, namely when the fatigue crack advanced 3 mm after precracking had been completed.

TABLE 1
DESIGN OF THE FATIGUE CRACK GROWTH TESTS

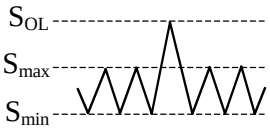

Specimen No.	Stress ratio R	Thickness t (mm)	Test type	Stress levels (MPa)		
				S_{min}	S_{max}	S_{OL}
0205	0	4	CA	4.3	84.3	—
0206	0.5	4	CA	80	160	—
0211	0.7	4	CA	116.67	166.67	—
0202	0	12	CA	4.3	84.3	—
0205	0.5	12	CA	80	160	—
0212	0.7	12	CA	116.67	166.67	—
0213	0	18	CA	4.06	79.62	—
0210	0	4	VA	4.3	84.3	164.3
0209	0.5	4	VA	80	160	240
0208	0	12	VA	4.3	84.3	164.3
0207	0.5	12	VA	80	160	240
0214	0	18	VA	4.06	79.62	155.17

The crack length was monitored with an accuracy of ±0.02 mm by a direct current potential drop method and visually, employing a travelling microscope. Fatigue fracture surfaces were observed macroscopically and microscopically in SEM in order to see the crack front marking of the OL and to reveal possible striations.

FATIGUE TEST RESULTS

The crack growth curves from all tests are plotted in Fig 2 where *N* denotes number of cycles after precracking. It is clear that the OL cycles introduced crack growth retardation in all tests and that the retardation effect at a given *R*-ratio decreased as specimen thickness was increased. Under CA loading conditions, however, the influence of *t* was negligible.

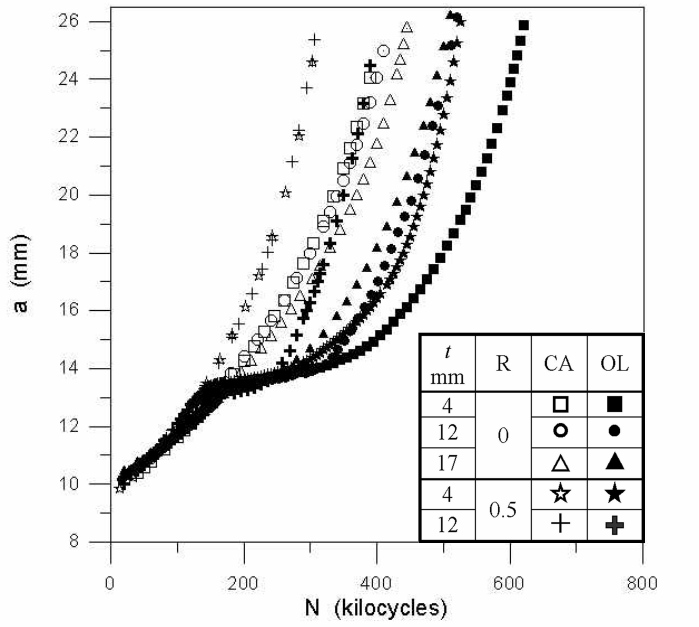

Figure 2: Crack growth curves from all fatigue tests

An incremental polynomial method using a 7-point fit was employed to compute the fatigue crack growth rate (FCGR) from the data presented in Fig. 2. The results are shown in Figs 3 and 4 by plotting the FCGR (d*a*/d*N*) as a function of crack length (*a*). As seen in Figs 3a and b, a thinner specimen always shows more retardation than a thicker specimen at the same *R*-ratio. The above trend is more pronounced when specimen thicknesses of 4 mm and 12 mm are considered whereas only minor differences can be noted between the behaviour of the 12 mm thick and 18 mm thick specimens. The thickness effect is more significant at R = 0.5 (Fig. 3b) than at R = 0 (Fig. 3a).

It is apparent in Fig. 4a that the retarded FCGRs observed in the R = 0 and R = 0.5 test on the 4 mm thick specimens coincide, except at highest values of *a*. This behaviour is in contrast to that shown in Fig. 4b by the 12 mm thick specimens. Here the FCGRs recover slower from the minimum d*a*/d*N* value at R = 0 than at R = 0.5.

The magnitude of the instantaneous load interaction effect after an OL can be represented by the FCGR observed in the OL test, $(da/dN)_{OL}$, normalized by the FCGR measured in the CA test at the same crack length for the same specimen thickness and *R*-ratio, $(da/dN)_{CA}$. It can be seen in Fig. 5 where the $(da/dN)_{OL}/(da/dN)_{CA}$ ratios from all the tests are plotted against the post-OL crack increment ($a - a_{OL}$) that the initial acceleration following an OL application only occurred in the R = 0 tests on the 4 mm thick and 12 mm thick specimen. This is also evident in Figs 3a where the d*a*/d*N* values measured in the above mentioned two tests jump immediately after the OL above the level observed in the corresponding CA tests. Fig. 5 further shows that the minimum in FCGRs is always attained when the crack has grown some distance after an OL. This implies that the so called delayed retardation occurred under all test conditions. The a-a_{OL} crack

growth increment corresponding to the minimum post-OL da/dN value was nearly the same in all tests (0.38 - 0.51 mm), as also was the minimum $(da/dN)_{OL}/(da/dN)_{CA}$ ratio (0.08 - 0.12 except of a higher value of 0.33 for the 18 mm thick specimen). From Fig. 5, for specimen thickness of 4 mm, more retardation occurred at $R = 0.5$ than at $R = 0$. A conspicuous feature observed in Fig. 5 for the larger thicknesses and also apparent in Figs 3 and 4 is accelerated crack growth following the retardation phase. This effect is most pronounced for the 18 mm thick specimen.

The overall retardation effect induced by an OL can be quantified using the measures shown in Fig. 6, namely the delay period (defined alternatively as N_D' or N_D'') and the delay distance also referred to as the OL-affected zone (Δa_{OL}). The normalized N_D''/N_{CA} parameter seems to be a more realistic measure of the amount of retardation than N_D' or N_D'', as it quantifies the benefit from applying an OL under given test conditions.

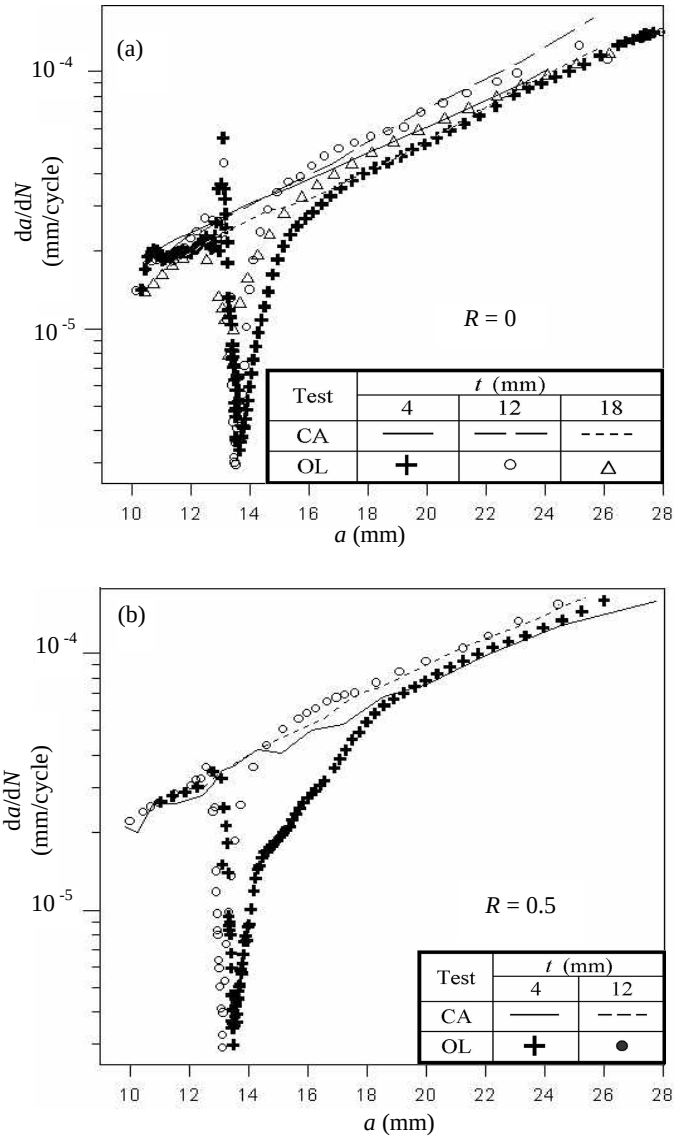

Figure 3: The effect of specimen thickness on post-OL crack growth rates: (a) at $R = 0$; (b) at $R = 0.5$

The observed effects of t and R on the retardation parameters depicted in Fig. 6 are summarized in Figs 7a and b. The N_D' vs. t data in Fig. 7a confirm the trend also visible in Fig. 2: increasing specimen thickness reduces the delay period. When the test results are viewed in terms of N_D''/N_{CA} vs. t it is apparent that larger profits from the OL application have been gained at $R = 0.5$ than at $R = 0$. At $R = 0$ the OLs brought about

equally beneficial results for the 4 mm thick and the 12 mm thick specimen (same N_D''/N_{CA} values), whilst for the 18 mm thick specimen the OL effect on crack growth was dramatically smaller.

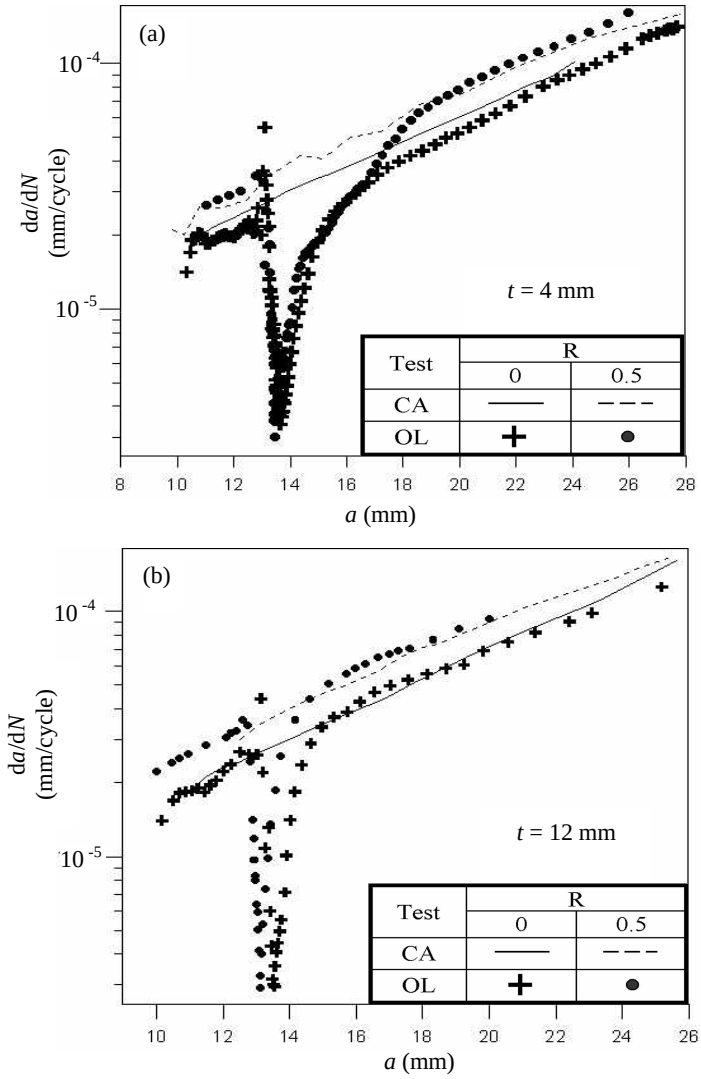

Figure 4: The effect of stress ratio on post-OL crack growth rates: (a) in 4 mm thick specimens; (b) in 12 mm thick specimens

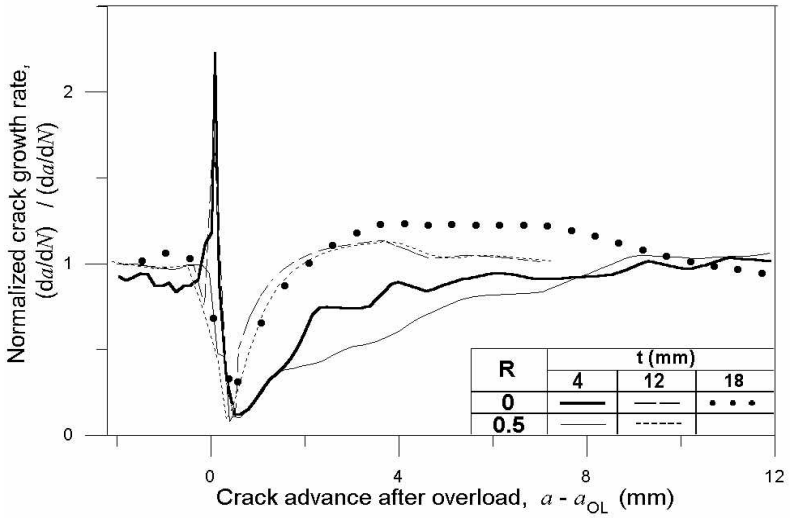

Figure 5: Variations of normalized crack growth rates throughout the OL tests

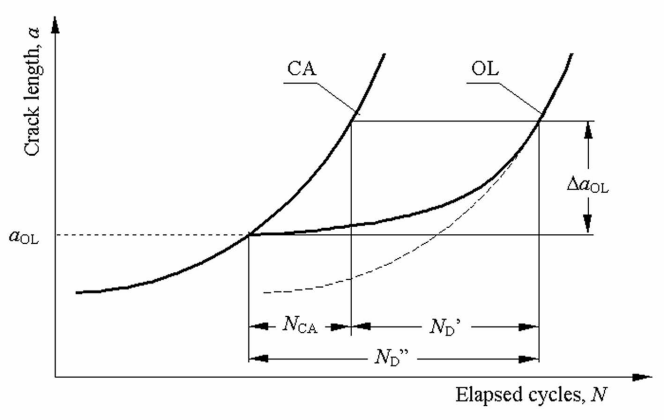

Figure 6: Definition of parameters to quantify the retardation effect

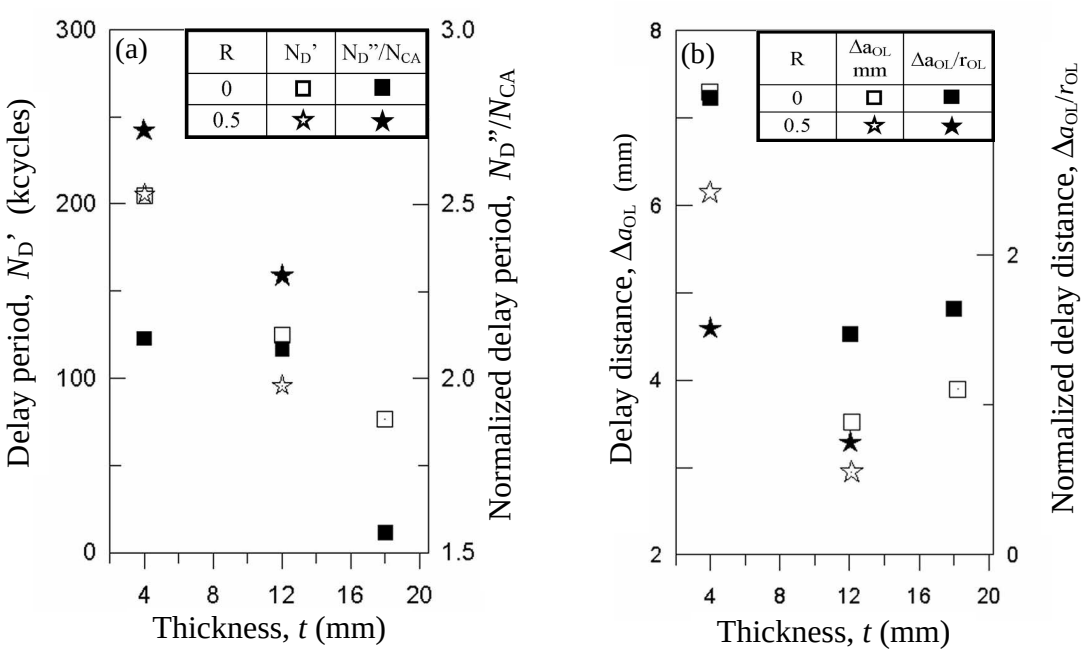

Figure 7: The effects of specimen thickness and stress ratio on: (a) delay period; (b) OL-affected zone

In terms of Δa_{OL}, the most effective was an OL applied on the 4 mm thick specimen in the $R = 0$ test, Fig. 7b. The Δa_{OL} vs. t data further show that delay distances observed at $R = 0$ for 12 mm and 18 mm specimen thickness are similar. A normalized parameter often cited in the literature, e.g.[2-4], is $\Delta a_{OL}/r_{OL}$, where r_{OL} is the OL plastic zone size. The $\Delta a_{OL}/r_{OL}$ vs. t data with r_{OL} computed for plane stress conditions show similar tendencies as the Δa_{OL} vs. t data, Fig. 7b. Note that at $R = 0$ the delay distances exceed the corresponding plastic zone sizes, i.e. $\Delta a_{OL}/r_{OL} > 1$, even for the thicker specimens.

Results generated on structural steels show that an increase of specimen thickness reduces the retardation phenomenon, both in terms of the delay period and the OL-affected zone [2,3], which is in agreement with the present work (see Fig. 7). However, Shuter and Geary [3] obtained a linear relationship between log N_D'' and t. It implies a more significant effect of thickness on the delay period than seen in Fig. 7a. As recognized by Fleck [2], Δa_{OL} measured on the surface of thinner specimens at $R = 0$ can significantly exceed r_{OL}, whereas Δa_{OL} measured on the surface of thick specimens is always smaller than r_{OL} [2,3]. In the present tests, however, Δa_{OL} at $R = 0$ was in all cases greater than r_{OL} (Fig. 7b). Investigations [2,3] indicated that an increase of specimen thickness caused the minimum in da/dN to occur earlier and become less deep. In contrast, Figs 3 and 5 demonstrate that both the minimum da/dN value and the distance at which this

minimum is reached do not depend on thickness. It is apparent that specimen thickness affects retardation only in the stage when FCGRs are recovering from the minimum value.

Systematic investigations on *R*-ratio effects on post-OL crack growth transients in structural steels are lacking in the literature. Shin and Hsu [4] noted the normalized minimum FCGR in stainless steel to become higher and Δa_{OL} to decrease as the *R*-ratio was increased. Only the latter trend is in accordance with the present results, Fig. 7b. The ratio of the minimum d*a*/d*N* position from point of OL to OL-affected zone ranges in our tests from 0.05 to 0.15 which is much lower than most of the values which can be estimated from test data presented in other works [2-4].

In contrast to the present work, all literature results cited above have been obtained from *K*-controlled tests on CT specimens. Hence, the differences between the post-OL crack growth behaviour observed here and that reported by others may stem not only from material related aspects but also from the different loading conditions and specimen geometry.

FRACTOGRAPHY

The macroscopic examination of the fatigue fracture surfaces indicated that each OL cycle produced a marking line which was vaguely visible only. It was slightly curved, i.e. the crack length at mid thickness was larger than at the specimen surface, a difference in the order of 0.5 mm. Curved crack fronts corresponding to OL cycles were also reported by Matsuoka and Tanaka [5]. Shear lips, typically observed for aluminium alloys [6] and also for a high strength steel [5], were not formed.

An OL marking line observed in the SEM was rather tortuous, and at a high magnification could not always be followed continuously over the full thickness of the specimen, Fig. 8. Close to the specimen surface, the OL marker lines could not be observed any more. A tentative explanation is that these lines may have been erased due to enhanced closure in the „plane stress" regions near the specimen surfaces. The fatigue fracture surfaces showed a rather irregular pattern with tortuous lines, as also evident for a low carbon steel (0.18C, 0.92Mn) from a SEM examination by Shuter and Geary [3]. No striations of the base line fatigue load cycles were found in the SEM. Apparently, the corresponding FCGR (in the range of 0.01 – 0.1 μm/cycle) was too low to lead to an easy detection in the SEM for this type of steel. In this respect, fatigue fracture surfaces of cracks in Al-alloys can be more instructive because they usually show many striations. Also, the correlation between a variable amplitude load history and the striation pattern has been found to be most useful [6].

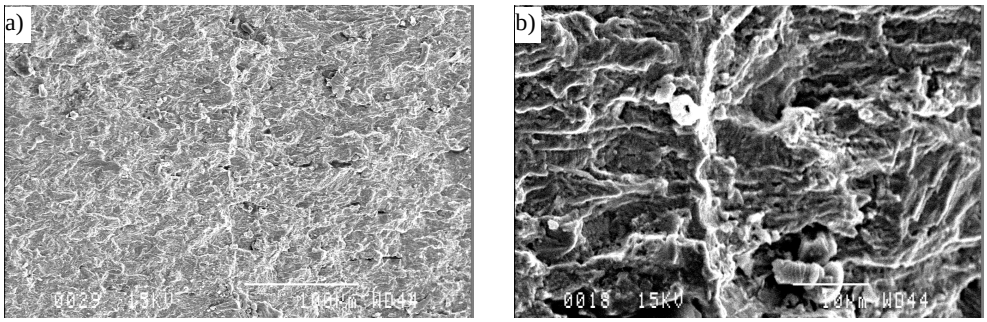

Figure 8: SEM micrographs of the fracture surface of Specimen 0207 at the OL position: (a) at a lower and (b) at a higher magnification. Vertically, in the centre of both pictures the crack front of the OL

ACKNOWLEDGEMENTS

The authors would like to acknowledge the partial financial support of the State Committee for Scientific Research via Grant No. PB 1459/T07/97/12.

REFERENCES

1. Skorupa M. (1998) Fatigue Fract. Engng Mater. Struct. **21**, 987.
2. Fleck N.A. (1988) ASTM STP **924**, vol. 1, 157.
3. Shuter D.M. and Geary W. (1996) Fatigue Fract. Engng Mater. Struct. **19**, 185.
4. Shin C.S. and Hsu S.H.(1993) Int. J. Fatigue **15**, 181.
5. Matsuoka S. and Tanaka K. (1980) Engng Fracture Mech. **13**, 293.
6. Schijve J. (1999) Fatigue Fract. Engng Mater. Struct. **22**, 87.